Preprints of the 19th World Congress
The International Federation of Automatic Control
Cape Town, South Africa. August 24-29, 2014

Discrete-time Switching MIMO LPV Gain-scheduling Control for the Reduction of Engine-induced Vibrations in Vehicles

Pablo Ballesteros, Xinyu Shu and Christian Bohn

Institute of Electrical Information Technology, Clausthal University of Technology, Germany,
(e-mail: ballesteros@iei.tu-clausthal.de, shu@iei.tu-clausthal.de, bohn@iei.tu-clausthal.de).

Abstract: The work of this paper is an extension of the previous work realized by the authors. The main objective of this work is the reduction of the engine-induced vibrations in vehicles using a switching strategy to augment the controller range of actuation. Two inertia mass actuators and two accelerometers are attached to the engine mounts. Multiple input multiple output (MIMO) linear parameter-varying (LPV) controllers are designed for the reduction of the engine-induced vibrations and validated experimentally with test drives in a Golf VI Variant. The stability of the controllers is guaranteed since LPV gain-scheduling techniques are used. The MIMO LPV controllers achieved excellent results for the reduction of nine frequency components of the engine-induced vibration using only two gain-scheduling parameters for a range of 750 rpm.

1. INTRODUCTION

Noise, vibration and harshness characteristics of cars and trucks are becoming increasingly important in recent years (Bein et al. (2012), Bohn et al. (2003, 2004), Duan et al. (2013), Inoue et al. (2004), Matsuoka et al. (2004), Sano et al. (2001, 2002), Soureshi and Knurek (1996), Shoureshi et al. (1997) and Svaricek et al. (2010)). The work presented here focuses on the reduction of the engine-induced vibrations through switching between multiple input multiple output (MIMO) linear parameter-varying (LPV) gain-scheduling controllers.

The use of adaptive methods for the reduction of vibration is the classical approach in active noise and vibration control (ANC/AVC). Adaptive filtering updating the filter coefficients through the Filtered-x LMS (FxLMS) is the technique commonly applied (Inoue et al. (2004), Matsuoka et al. (2004), Sano et al. (2001, 2002), Soureshi and Knurek (1996), Shoureshi et al. (1997) and Svaricek et al. (2010)). An analysis of the closed loop using adaptive techniques is difficult since the filter weights are the result of an adaptation. The stability and transient behavior (convergence speed) depend on the system input. Also, to the best of the authors' knowledge, only “approximate stability results” are available for the FxLMS algorithm (Feintuch et al. (1993)).

LPV gain-scheduling techniques can be used for the rejection of harmonic disturbances (Ballesteros and Bohn (2011a, 2011b), Ballesteros et al. (2012, 2013, 2014a, 2014b), Darengosse and Chevrel (2000), Du and Shi (2002), Du et al. (2003), Füger et al. (2012, 2013), Heins et al. (2011, 2012a, 2012b), Kinney and Callafon (2006), Köroğlu and Scherer (2008), Shu et al. (2011, 2013a, 2013b) and Witte et al. (2010)). The use of these techniques guarantees the stability for changes in the gain-scheduling parameters. This is the main advantage of the LPV design techniques compared with the adaptive techniques. In this paper LPV gain-scheduling techniques are used for the rejection of harmonic disturbances since the engine-induced vibrations are of this kind.

The work presented in this paper is an extension of the previous work realized by the authors and particularly an extension of the MIMO LPV controller presented in Ballesteros et al. (2014a, 2014b). In this paper a switching MIMO LPV control strategy is used to augment the actuation range of the controllers guaranteeing the stability in the switching instant. Two inertia mass actuators (shakers) and two accelerometers are attached to the engine mounts. The controller uses the measurements of the accelerometers to generate the cancelling signal of the shakers. Anti-aliasing filters are applied to the output signals and reconstruction filters to the control inputs. The controllers are designed for the rejection of nine frequency components and are implemented on a rapid prototyping unit (MicroAutoBox from dSPACE). The switching strategy is validated with test drives for two MIMO LPV controllers covering a range of 750 rpm with only two gain-scheduling parameters.

The remainder of this paper is organized as follows. The MIMO LPV control design for the rejection of the engine-induced vibrations is presented in Sec. 2. The switching strategy to augment the range of reduction for the controller is explained in Sec. 3. Experiments in test drives with a Golf VI Variant are shown in Sec. 4. In Sec. 5 some summary and conclusions are given.

2. CONTROL DESIGN

The disturbance-observer state-feedback controller for the rejection of harmonic disturbances of Bohn et al. (2003, 2004) is reviewed in the following and extended to an LPV control structure. This controller is based on the internal model principle of Francis and Wonham (1976). To achieve disturbance rejection the controller contains a model of the disturbance. The disturbances are time varying and therefore LPV gain-scheduling techniques are used to guarantee the stability. In subsection 2.1 an LPV state-space representation of the engine-induced vibrations is obtained. The control structure is briefly explained in subsection 2.2 and the LPV controller is calculated in subsection 2.3.

2.1. LPV Disturbance Modeling

The harmonic vibrations generated by the engine can be modeled as the output

$$\begin{aligned} \boldsymbol{x}_{\mathrm{d},k+1} &= \boldsymbol{A}_{\mathrm{d},k}\boldsymbol{x}_{\mathrm{d},k}, \\ \boldsymbol{y}_{\mathrm{d},k} &= \boldsymbol{C}_{\mathrm{d}}\boldsymbol{x}_{\mathrm{d},k} \end{aligned} \tag{1}$$

of an $n \times n$ MIMO harmonic disturbance model for n_{d} time-varying frequencies with

$$\boldsymbol{A}_{\mathrm{d},k} = \begin{bmatrix} \boldsymbol{A}_{\mathrm{d}_1,k} & \cdots & \boldsymbol{0} \\ \vdots & \ddots & \vdots \\ \boldsymbol{0} & \cdots & \boldsymbol{A}_{\mathrm{d}_n,k} \end{bmatrix}, \tag{2}$$

$$\boldsymbol{A}_{\mathrm{d}_1,k} = \cdots = \boldsymbol{A}_{\mathrm{d}_n,k} = \begin{bmatrix} \tilde{\boldsymbol{A}}_{\mathrm{d}_1,k} & \cdots & \boldsymbol{0} \\ \vdots & \ddots & \vdots \\ \boldsymbol{0} & \cdots & \tilde{\boldsymbol{A}}_{\mathrm{d}_{n_\mathrm{d}},k} \end{bmatrix}, \tag{3}$$

$$\tilde{\boldsymbol{A}}_{\mathrm{d}_i,k} = \begin{bmatrix} r\cos(\Omega_{i,k}) & r\sin(\Omega_{i,k}) \\ -r\sin(\Omega_{i,k}) & r\cos(\Omega_{i,k}) \end{bmatrix}, \Omega_{i,k} = 2\pi f_{i,k} T, \tag{4}$$

$f_{i,k} \in [f_{i,\min}, f_{i,\max}]$ for $i = 1, \ldots, n_{\mathrm{d}}$ and

$$\boldsymbol{C}_{\mathrm{d}} = \begin{bmatrix} \boldsymbol{C}_{\mathrm{d}_1} & \cdots & \boldsymbol{0} \\ \vdots & \ddots & \vdots \\ \boldsymbol{0} & \cdots & \boldsymbol{C}_{\mathrm{d}_n} \end{bmatrix}, \boldsymbol{C}_{\mathrm{d}_1} = \cdots = \boldsymbol{C}_{\mathrm{d}_n} = \begin{bmatrix} 1 \ 0 \cdots 1 \ 0 \end{bmatrix}. \tag{5}$$

A classical LPV representation can be obtained for this model using $r\cos(\Omega_{i,k})$ and $r\sin(\Omega_{i,k})$ as time-varying parameters. This approach leads to an LPV model with $2n_{\mathrm{d}}$ parameters even in the case where the frequencies are harmonically related.

To reduce the number of parameters in the case where the frequencies are harmonically related, a useful idea is proposed by Füger et al. (2012, 2013) which allows a formulation of this model in LPV form with only two parameters, independently of the number of disturbance frequencies. Füger et al. (2012, 2013) used a polynomial approximation to reduce the number of gain-scheduling parameters for a single input single output (SISO) model of constant frequencies.

In the work presented in this paper, the polynomial approximation is used for an MIMO model with time-varying frequencies. The sine function and the cosine function can be written as

$$r\sin(\Omega_{i,k}) \approx a_{i,0} + a_{i,1}\Omega_{0,k} + \ldots + a_{i,N_\mathrm{p}}\Omega_{0,k}^{N_\mathrm{p}} \tag{6}$$

$$r\cos(\Omega_{i,k}) \approx b_{i,0} + b_{i,1}\Omega_{0,k} + \ldots + b_{i,N_\mathrm{p}}\Omega_{0,k}^{N_\mathrm{p}} \tag{7}$$

for n_{d} harmonically related time-varying frequencies

$$\boldsymbol{f}_k = \left[f_{1,k}, f_{2,k}, \ldots, f_{n_\mathrm{d},k}\right] = \left[h_1, h_2, \ldots, h_{n_\mathrm{d}}\right] f_{0,k}. \tag{8}$$

A least square fit can be used to calculate the constant coefficients $a_{i,0}, \ldots, a_{i,N_\mathrm{p}}$ and $b_{i,0}, \ldots, b_{i,N_\mathrm{p}}$ for all the frequencies of the disturbance for a given range of the fundamental frequency $f_{0,k} \in [f_{0,\min}, f_{0,\max}]$. Simulations and experiments achieved a very good approximation with only three coefficients. Therefore here the sine and cosine function are approximated as

$$r\sin(\Omega_{i,k}) \approx a_{i,0} + a_{i,2}\Omega_{0,k}^2 + a_{i,4}\Omega_{0,k}^4 \tag{9}$$

$$r\cos(\Omega_{i,k}) \approx b_{i,0} + b_{i,2}\Omega_{0,k}^2 + b_{i,4}\Omega_{0,k}^4. \tag{10}$$

The time-varying parameters

$$\theta_{1,k} = \Omega_{0,k}^2 = (2\pi f_{0,k} T)^2, \tag{11}$$

$$\theta_{2,k} = \Omega_{0,k}^4 = (2\pi f_{0,k} T)^4 \tag{12}$$

are introduced and the matrix $\tilde{\boldsymbol{A}}_{\mathrm{d}_i,k}$ can be written as

$$\tilde{\boldsymbol{A}}_{\mathrm{d}_i,k} \approx \begin{bmatrix} a_{i,0} & b_{i,0} \\ -b_{i,0} & a_{i,0} \end{bmatrix} + \begin{bmatrix} a_{i,2} & b_{i,2} \\ -b_{i,2} & a_{i,2} \end{bmatrix}\theta_{1,k} + \begin{bmatrix} a_{i,4} & b_{i,4} \\ -b_{i,4} & a_{i,4} \end{bmatrix}\theta_{2,k} \tag{13}$$

with only two gain-scheduling parameters independently of the number of frequencies. An LPV representation of the matrix $\boldsymbol{A}_{\mathrm{d},k}$ with two gain-scheduling parameters is possible since the matrices $\tilde{\boldsymbol{A}}_{\mathrm{d}_i,k}$ are included in the matrix $\boldsymbol{A}_{\mathrm{d},k}$.

2.2. Control Structure

In this subsection the disturbance-observer state-feedback control structure for the rejection of harmonic disturbances is introduced. According to the internal model principle, the controller contains the model of the disturbance to be rejected. The LPV disturbance model for harmonic disturbances of the previous section is used since the engine-induced vibrations are time varying. The dynamics of the LPV disturbance are included in the controller using state augmentation.

The control structure is a state-feedback gain combined with an identity observer of an augmented system. The augmented system is obtained with a disturbance modeled as the output of (1) acting at the input of the plant. A state-space representation of the plant is given by

$$\begin{aligned} \boldsymbol{x}_{\mathrm{p},k+1} &= \boldsymbol{A}_{\mathrm{p}}\boldsymbol{x}_{\mathrm{p},k} + \boldsymbol{B}_{\mathrm{p}}\left(\boldsymbol{u}_{\mathrm{p},k} + \boldsymbol{y}_{\mathrm{d},k}\right), \\ \boldsymbol{y}_{\mathrm{p},k} &= \boldsymbol{C}_{\mathrm{p}}\boldsymbol{x}_{\mathrm{p},k}. \end{aligned} \tag{14}$$

For the control design, plant and disturbance are combined to obtain the augmented system given as

$$\begin{aligned} \begin{bmatrix} \boldsymbol{x}_{\mathrm{d},k+1} \\ \boldsymbol{x}_{\mathrm{p},k+1} \end{bmatrix} &= \begin{bmatrix} \boldsymbol{A}_{\mathrm{d},k} & \boldsymbol{0} \\ \boldsymbol{B}_{\mathrm{p}}\boldsymbol{C}_{\mathrm{d}} & \boldsymbol{A}_{\mathrm{p}} \end{bmatrix} \begin{bmatrix} \boldsymbol{x}_{\mathrm{d},k} \\ \boldsymbol{x}_{\mathrm{p},k} \end{bmatrix} + \begin{bmatrix} \boldsymbol{0} \\ \boldsymbol{B}_{\mathrm{p}} \end{bmatrix}\boldsymbol{u}_{\mathrm{p},k}, \\ \boldsymbol{y}_{\mathrm{p},k} &= \begin{bmatrix} \boldsymbol{0} & \boldsymbol{C}_{\mathrm{p}} \end{bmatrix} \begin{bmatrix} \boldsymbol{x}_{\mathrm{d},k} \\ \boldsymbol{x}_{\mathrm{p},k} \end{bmatrix} \end{aligned} \tag{15}$$

and it can be written in compact form as

$$\begin{aligned} \boldsymbol{x}_{k+1} &= \boldsymbol{A}_k\boldsymbol{x}_k + \boldsymbol{B}\boldsymbol{u}_{\mathrm{p},k}, \\ \boldsymbol{y}_{\mathrm{p},k} &= \boldsymbol{C}\,\boldsymbol{x}_k \end{aligned} \tag{16}$$

with $\boldsymbol{x}_k = \begin{bmatrix} \boldsymbol{x}_{\mathrm{d},k} \\ \boldsymbol{x}_{\mathrm{p},k} \end{bmatrix}, \boldsymbol{A}_k = \begin{bmatrix} \boldsymbol{A}_{\mathrm{d},k} & \boldsymbol{0} \\ \boldsymbol{B}_{\mathrm{p}}\boldsymbol{C}_{\mathrm{d}} & \boldsymbol{A}_{\mathrm{p}} \end{bmatrix}, \boldsymbol{B} = \begin{bmatrix} \boldsymbol{0} \\ \boldsymbol{B}_{\mathrm{p}} \end{bmatrix}$ and $\boldsymbol{C} = \begin{bmatrix} \boldsymbol{0} & \boldsymbol{C}_{\mathrm{p}} \end{bmatrix}$.

The control structure is a state-feedback gain of the augmented system

$$\boldsymbol{u}_{\mathrm{p},k} = -\boldsymbol{K}\,\hat{\boldsymbol{x}}_k = -\begin{bmatrix} \boldsymbol{K}_{\mathrm{d}} & \boldsymbol{K}_{\mathrm{p}} \end{bmatrix} \begin{bmatrix} \hat{\boldsymbol{x}}_{\mathrm{d},k} \\ \hat{\boldsymbol{x}}_{\mathrm{p},k} \end{bmatrix} \tag{17}$$

with the estimated states $\hat{\boldsymbol{x}}_k$ calculated through an identity observer

$$\hat{\boldsymbol{x}}_{k+1} = \left(\boldsymbol{A}_k - \boldsymbol{L}_k\boldsymbol{C}\right)\hat{\boldsymbol{x}}_k + \boldsymbol{B}\boldsymbol{u}_{\mathrm{p},k} + \boldsymbol{L}_k\boldsymbol{y}_{\mathrm{p},k} \tag{18}$$

of the augmented system. It can be shown in Heins et al. (2012) that as long as a stabilizing state-feedback gain $\boldsymbol{K}_{\mathrm{p}}$ for the LTI plant and a stabilizing observer gain $\boldsymbol{L}_k$ are found, the overall closed-loop system is stable. The state-feedback gain $\boldsymbol{K}_{\mathrm{d}}$ for the disturbance model has no effect on the stability of the closed loop (as long as $\boldsymbol{K}_{\mathrm{d}}\hat{\boldsymbol{x}}_{\mathrm{d},k}$ remains bounded). Disturbance rejection is achieved with $\boldsymbol{K}_{\mathrm{d}} = \boldsymbol{C}_{\mathrm{d}}$.

Finally, a state-space representation of the controller is given by

$$\begin{aligned} \boldsymbol{x}_{\mathrm{c},k+1} &= \boldsymbol{A}_{\mathrm{c},k}\boldsymbol{x}_{\mathrm{c},k} + \boldsymbol{B}_{\mathrm{c},k}\boldsymbol{y}_{\mathrm{p},k}, \\ \boldsymbol{u}_{\mathrm{p}} &= \boldsymbol{C}_{\mathrm{c}}\boldsymbol{x}_{\mathrm{c},k} \end{aligned} \tag{19}$$

with

$$\boldsymbol{A}_{\mathrm{c},k} = \boldsymbol{A}_k - \boldsymbol{L}_k\boldsymbol{C} - \boldsymbol{B}\boldsymbol{K}, \tag{20}$$

$\boldsymbol{B}_{\mathrm{c},k} = \boldsymbol{L}_k$ and $\boldsymbol{C}_{\mathrm{c}} = -\boldsymbol{K}$.

2.3. pLPV Controller Design

It can be seen from (13) and (16) that the matrix $\boldsymbol{A}_k$ of the augmented system depends on the parameters $\theta_{1,k}$ and $\theta_{2,k}$. Powerful control design methods can be used if the parameters $\theta_{1,k}$ and $\theta_{2,k}$ vary inside a polytope. Since the relationship between the parameters is known

$$\theta_{2,k} = \theta_{1,k}^2, \tag{21}$$

a triangle as polytope is in this paper used.

The two scheduling parameters $\theta_{1,k} = \Omega_{1,k}^2$ and $\theta_{2,k} = \Omega_{1,k}^4$ vary for a fundamental frequency $f_{0,k} \in \left[f_{0,\min}, f_{0,\max}\right]$ inside a triangle in $\mathbb{R}^2$ with vertices

$$\begin{aligned} \bar{\boldsymbol{\theta}}_1 &= [\theta_{1,\min} \quad \theta_{1,\min}^2]^{\mathrm{T}}, \\ \bar{\boldsymbol{\theta}}_2 &= [(\theta_{1,\min} + \theta_{1,\max})/2 \quad \theta_{1,\min}\theta_{1,\max}]^{\mathrm{T}}, \\ \bar{\boldsymbol{\theta}}_3 &= [\theta_{1,\max} \quad \theta_{1,\max}^2]^{\mathrm{T}}, \\ \theta_{1,\min} &= (2\pi f_{0,\min}T)^2 \end{aligned} \tag{22}$$

and $\theta_{1,\max} = (2\pi f_{0,\max}T)^2$ as shown in Fig. 1.

The time-varying system matrix $\boldsymbol{A}_k$ of the augmented system depend affinely on the parameters $\boldsymbol{\theta}_k = \begin{bmatrix} \theta_{1,k} & \theta_{2,k} \end{bmatrix}^{\mathrm{T}} \in \Theta \subset \mathbb{R}^2$

$$\boldsymbol{A}_k = \boldsymbol{A}(\boldsymbol{\theta}_k) = \boldsymbol{\mathcal{A}}_0 + \theta_{1,k}\boldsymbol{\mathcal{A}}_1 + \theta_{2,k}\boldsymbol{\mathcal{A}}_2 \tag{23}$$

where the matrices $\boldsymbol{\mathcal{A}}_0$, $\boldsymbol{\mathcal{A}}_1$ and $\boldsymbol{\mathcal{A}}_2$ are constant matrices and Θ is a convex polytope with vertices $\bar{\boldsymbol{\theta}}_1, \bar{\boldsymbol{\theta}}_2, \bar{\boldsymbol{\theta}}_3 \in \Theta \subset \mathbb{R}^2$. Then, an arbitrary point $\boldsymbol{\theta}_k$ inside the polytope can be written as a convex combination of the three vertices with a time-varying coordinate vector $\boldsymbol{\lambda}_k = \begin{bmatrix} \lambda_{1,k} & \lambda_{2,k} & \lambda_{3,k} \end{bmatrix}^{\mathrm{T}} \in \mathbb{R}^3$ via

$$\lambda_{j,k} \geq 0, \ \sum_{j=1}^{3} \lambda_{j,k} = 1 \text{ and } \boldsymbol{\theta}_k = \sum_{j=1}^{3} \lambda_{j,k}\,\bar{\boldsymbol{\theta}}_j. \tag{24}$$

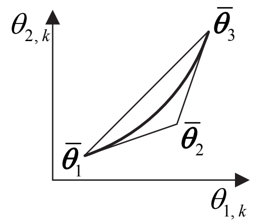

Fig 1. Triangle as a polytope in $\mathbb{R}^2$.

The parameter $\boldsymbol{\theta}_k$ is obtained with (24) and the coordinate vector $\boldsymbol{\lambda}_k$ is calculated through

$$\begin{bmatrix} \lambda_{1,k} \\ \lambda_{2,k} \\ \lambda_{3,k} \end{bmatrix} = \begin{bmatrix} \bar{\boldsymbol{\theta}}_1 & \bar{\boldsymbol{\theta}}_2 & \bar{\boldsymbol{\theta}}_3 \\ 1 & 1 & 1 \end{bmatrix}^{-1} \begin{bmatrix} \theta_{1,k} \\ \theta_{2,k} \\ 1 \end{bmatrix}. \tag{25}$$

The inverse matrix can be calculated offline and then the calculation of the coordinate vector $\boldsymbol{\lambda}_k$ is the result of a matrix multiplication.

The matrix $\boldsymbol{A}_k$ depend on the parameters $\boldsymbol{\theta}_k = \begin{bmatrix} \theta_{1,k} & \theta_{2,k} \end{bmatrix}^{\mathrm{T}}$ and it can be written with (24) as

$$\boldsymbol{A}_k = \boldsymbol{A}(\boldsymbol{\theta}_k) = \boldsymbol{A}(\boldsymbol{\lambda}_k) = \lambda_{1,k}\boldsymbol{A}(\bar{\boldsymbol{\theta}}_1) + \cdots + \lambda_{3,k}\boldsymbol{A}(\bar{\boldsymbol{\theta}}_3) \tag{26}$$

with the coordinate vector $\boldsymbol{\lambda}_k$ calculated from (25) and the three linear time-invariant (LTI) vertex systems defined as $\boldsymbol{A}(\bar{\boldsymbol{\theta}}_j) = \boldsymbol{A}_{\mathrm{v},j}$ with $j = 1, \ldots, 3$.

The system based on this system matrix is regarded as a polytopic LPV (pLPV) system (16). With the augmented system written in this form, control design techniques are applied to obtain a pLPV gain-scheduling controller.

Three vertex observer gains $\boldsymbol{L}_{\mathrm{v},j}$ for the pLPV system are calculated for $\bar{\boldsymbol{\theta}}_j$ with $j = 1, \ldots, 3$ by solving linear matrix inequalities (LMIs) based on H_2 norm constraint guaranteeing quadratic stability. This procedure is briefly listed as follows.

Seven LMIs are solved for the variables $\boldsymbol{P}$, $\boldsymbol{W}$ and $\boldsymbol{Y}_{\mathrm{v},j}$

$$\begin{bmatrix} \boldsymbol{P} & \boldsymbol{P}\boldsymbol{A}_{\mathrm{v},j} - \boldsymbol{Y}_{\mathrm{v},j}^{\mathrm{T}}\boldsymbol{C} \\ \left(\boldsymbol{P}\boldsymbol{A}_{\mathrm{v},j} - \boldsymbol{Y}_{\mathrm{v},j}^{\mathrm{T}}\boldsymbol{C}\right)^{\mathrm{T}} & \boldsymbol{P} \end{bmatrix} > 0, \ j = 1, \ldots, 3, \tag{27}$$

$$\begin{bmatrix} \boldsymbol{W} & \tilde{\boldsymbol{Q}}\boldsymbol{P} - \tilde{\boldsymbol{R}}\boldsymbol{Y}_{\mathrm{v},j} \\ \left(\tilde{\boldsymbol{Q}}\boldsymbol{P} - \tilde{\boldsymbol{R}}\boldsymbol{Y}_{\mathrm{v},j}\right)^{\mathrm{T}} & \boldsymbol{P} \end{bmatrix} > 0, \ j = 1, \ldots, 3, \tag{28}$$

$$\operatorname{trace}\left(\boldsymbol{W}\right) < \gamma^2, \tag{29}$$

with

$$\tilde{\boldsymbol{Q}} = \begin{bmatrix} \boldsymbol{Q}^{\frac{\mathrm{T}}{2}} \\ \boldsymbol{0} \end{bmatrix}, \tilde{\boldsymbol{R}} = \begin{bmatrix} \boldsymbol{0} \\ \boldsymbol{R}^{\frac{\mathrm{T}}{2}} \end{bmatrix} \tag{30}$$

and $\boldsymbol{Y}_{\mathrm{v},j} = \boldsymbol{L}_{\mathrm{v},j}\boldsymbol{P},\ j = 1,\ldots,3.$ (31)

The vertex observer gains are calculated through

$$\boldsymbol{L}_{\mathrm{v},j} = \boldsymbol{P}^{-\mathrm{T}}\boldsymbol{Y}_{\mathrm{v},j}^{\mathrm{T}},\ j = 1,\ldots,3 .$$

In order to guarantee quadratic stability for the whole parameter space, solutions for the matrix variables $\boldsymbol{P}$ and $\boldsymbol{W}$ have to be the same for all vertex systems.

The controller in pLPV form with the calculated vertex observer gains is given by

$$\begin{aligned} \boldsymbol{x}_{\mathrm{c},k+1} &= \boldsymbol{A}_{\mathrm{c}}(\boldsymbol{\lambda}_k)\boldsymbol{x}_{\mathrm{c},k} + \boldsymbol{B}_{\mathrm{c}}(\boldsymbol{\lambda}_k)\boldsymbol{y}_{\mathrm{p},k}, \\ \boldsymbol{u}_{\mathrm{p},k} &= \boldsymbol{C}_{\mathrm{c}}\boldsymbol{x}_{\mathrm{c},k} \end{aligned} \tag{32}$$

with

$$\boldsymbol{A}_{\mathrm{c}}(\boldsymbol{\lambda}_k) = \left(\sum_{j=1}^{3}\lambda_{j,k}\left(\boldsymbol{A}_{\mathrm{v},j} - \boldsymbol{L}_{\mathrm{v},j}\boldsymbol{C}\right) - \boldsymbol{B}\boldsymbol{K}\right), \tag{33}$$

$$\boldsymbol{B}_{\mathrm{c}}(\boldsymbol{\lambda}_k) = \sum_{j=1}^{3}\lambda_{j,k}\boldsymbol{L}_{\mathrm{v},j} \tag{34}$$

and $\boldsymbol{C}_{\mathrm{c}} = -\boldsymbol{K}.$ (35)

The MIMO pLPV controller presented in this paper is very simple to implement. The controller is calculated from three controller vertices using a simple matrix multiplication.

3. SWITCHING CONTROL STRATEGY

The range of vibration reduction is augmented in this section by combining pLPV controllers. The main objective is to augment the range of vibration reduction guaranteeing the stability at the same time. As an approach, three triangles can be used as polytopes placed consecutively as shown in Fig. 2. The vertex gains $\boldsymbol{L}_{1,\boldsymbol{P}_1}$, $\boldsymbol{L}_{2,\boldsymbol{P}_1}$ and $\boldsymbol{L}_{3,\boldsymbol{P}_1}$ are calculated for the first triangle using the control design explained in the previous section. For the next triangle one vertex gain is fixed $\boldsymbol{L}_{3,\boldsymbol{P}_1} = \boldsymbol{L}_{1,\boldsymbol{P}_2}$ and two vertex gains are calculated solving the LMIs from (27-31) with $\boldsymbol{Y}_{\mathrm{v},1} = \boldsymbol{L}_{3,\boldsymbol{P}_1}\boldsymbol{P}$. The same procedure is carried out for further triangles.

This approach uses the same controller (same vertex gains) at each union point of the triangles. This switching strategy guarantees the stability if the parameters vary continuously. The stability is not guaranteed if the parameters vary from one triangle to another triangle region. For variations inside the triangle of the gain-scheduling parameters the stability is guaranteed. This approach was implemented in test drives and excellent results were achieved for three consecutive triangles covering a region of 1200 rpm for the reduction of nine frequency components of the engine-induced vibration.

The main objective is to switch between controllers guaranteeing the stability. Therefore an extension of this approach is realized finding a Lyapunov function $\boldsymbol{X}$ and solving the LMIs

$$\begin{bmatrix} \boldsymbol{X} & \boldsymbol{X}\left(\boldsymbol{A}_{\mathrm{v},j} - \boldsymbol{L}_{\mathrm{v},j}\boldsymbol{C} - \boldsymbol{B}\boldsymbol{K}\right) \\ \left(\boldsymbol{A}_{\mathrm{v},j} - \boldsymbol{L}_{\mathrm{v},j}\boldsymbol{C} - \boldsymbol{B}\boldsymbol{K}\right)^{\mathrm{T}}\boldsymbol{X} & \boldsymbol{X} \end{bmatrix} > 0 \tag{36}$$

for the vertex $j = 1,\ldots,4$ shown in Fig. 3. Quadratic stability is then guaranteed if a common Lyapunov function is found for the four vertex ($\boldsymbol{L}_{\mathrm{v},1} = \boldsymbol{L}_{1,\boldsymbol{P}_1}$, $\boldsymbol{L}_{\mathrm{v},2} = \boldsymbol{L}_{2,\boldsymbol{P}_1}$, $\boldsymbol{L}_{\mathrm{v},3} = \boldsymbol{L}_{2,\boldsymbol{P}_2}$, $\boldsymbol{L}_{\mathrm{v},4} = \boldsymbol{L}_{3,\boldsymbol{P}_2}$) of the polytope. A Lyapunov matrix $\boldsymbol{X}$ was found for a region of 750 rpm.

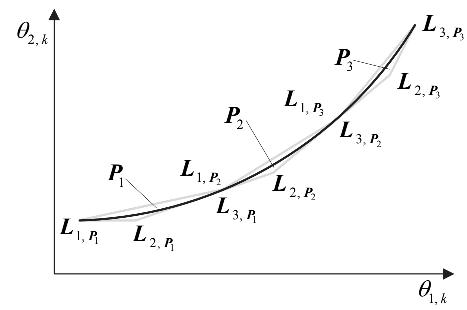

Fig. 2. Triangle division to switch between controllers.

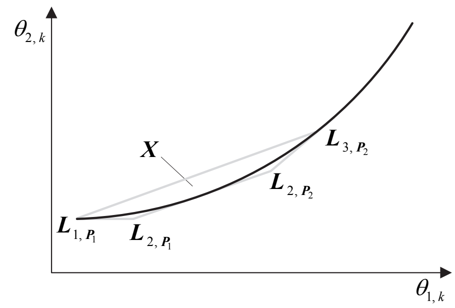

Fig. 3. Polygon to guarantee the stability of the controllers.

In a similar way as (25), the simple matrix multiplication to obtain the pLPV controller can be used if the polygon is further subdivided in triangles. A pLPV controller is used for the triangle ($\boldsymbol{L}_{1,\boldsymbol{P}_1}$, $\boldsymbol{L}_{2,\boldsymbol{P}_1}$, $\boldsymbol{L}_{2,\boldsymbol{P}_2}$) and another pLPV controller for the triangle ($\boldsymbol{L}_{2,\boldsymbol{P}_1}$, $\boldsymbol{L}_{2,\boldsymbol{P}_2}$, $\boldsymbol{L}_{3,\boldsymbol{P}_2}$). A switch between controllers is realized in the middle of the polygon and the controllers are initialized with the same state spaces. The stability is guaranteed since a common Lyapunov function was found for the four vertices and the switch is done between the vertices of the polytope.

4. EXPERIMENTAL RESULTS

Two 2×2 MIMO pLPV controllers obtained with the control design from Sec. 2 and the switching strategy of Sec. 3 are used for the reduction of the engine-induced vibrations in a Golf VI Variant. The controllers are designed to reject nine frequency components of the engine-induced vibration in a range of 750 rpm.

A schema of the experimental setup is shown in Fig. 4 and a photo in Fig. 5. Two inertia mass actuators (shakers) and two accelerometers to measure vertical accelerations are attached to the engine mounts. The battery is moved to the trunk of the car and the resulting space is used for the power amplifiers driving the actuators. The controllers generate the control signals for the shakers using the measurements of the accelerometers. Anti-aliasing filters are applied to the accelerometer signals and reconstruction filters to the control inputs. The filters and the rapid control prototyping unit were placed on the trunk of the car. All the cables between sensors and control unit and between actuators and control unit are hidden in the car body. The controllers are implemented on a rapid prototyping unit (MicroAutoBox from dSPACE) using a sampling frequency of 2 kHz.

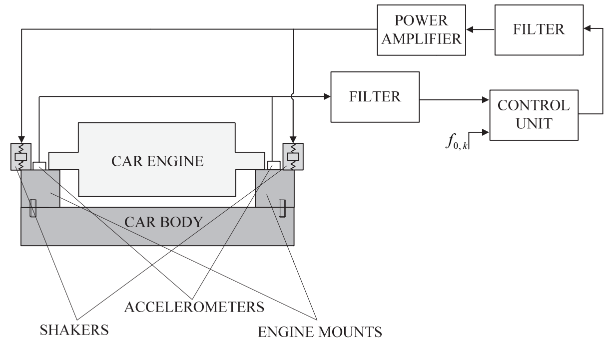

Fig. 4. Schema of the experimental setup.

Black-box system identification techniques are used to obtain a 2×2 MIMO state-space representation of the system between output and input of the control unit. The controllers are capable of reducing nine frequency components $f_{0,k}[4\ 5 \cdots 12]$ of the engine-induced vibration for a fundamental frequency (half engine order) $f_{0,k} \in [22.5, 28.75]$ Hz. The switch between the pLPV controllers is realized for a fundamental frequency of 25 Hz. Amplitude frequency responses in open loop and closed loop for a fundamental frequency of $f_{0,k} = 27,6$ Hz (engine speed of approximately 3320 rpm) are shown in Fig. 6.

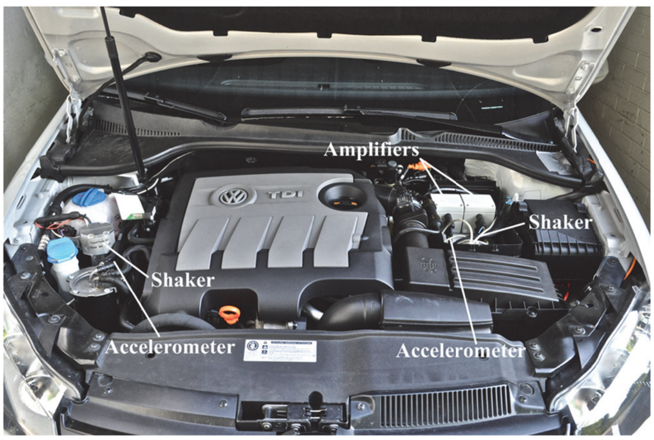

Fig. 5. Photo of the experimental setup.

The controllers were tested in drives with all the gears. In the following only results in third gear are shown. Results for an engine speed of approximately 3320 rpm are shown in Fig. 7 for a control sequence off/on/off. The spectrums of the accelerations are shown in Fig. 8. Excellent results were achieved for constant engine speeds as the spectrums of the acceleration in closed loop and open loop show.

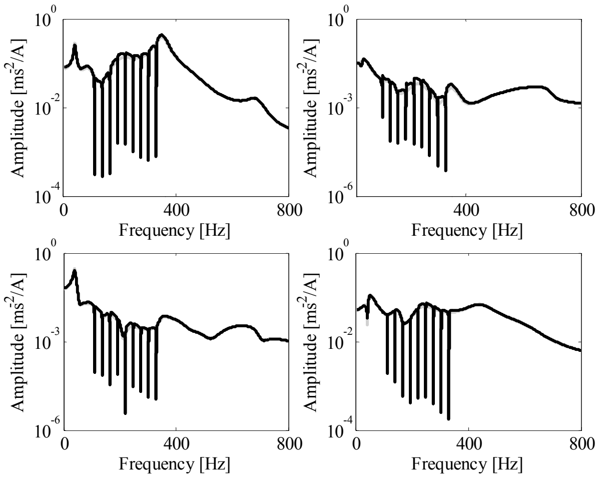

Fig. 6. Amplitude frequency responses in open loop (gray) and closed loop (black).

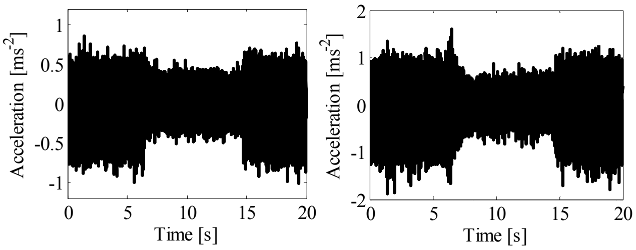

Fig. 7. Accelerations measured on the driver side (left) and rider side (right) for a control sequence off/on/off.

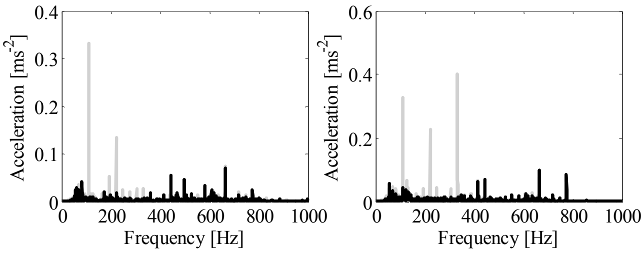

Fig. 8. Spectrums of the accelerations in open loop (gray) and closed loop (black) for the driver side (left) and rider side (right).

Further experiments were realized in test drives for the time-varying engine speed of Fig. 9. The accelerations measured on the driver and rider side are shown in Fig. 10. The controller is switched on for the first one hundred seconds and switched off for the next one hundred seconds.

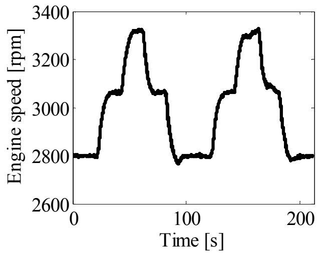

Fig. 9. Time-varying engine speed measured by the CAN bus.

Excellent results are achieved for the reduction of nine frequency components of the engine-induced vibration for time-varying engine speed as the time-frequency diagrams of Fig. 11 show.

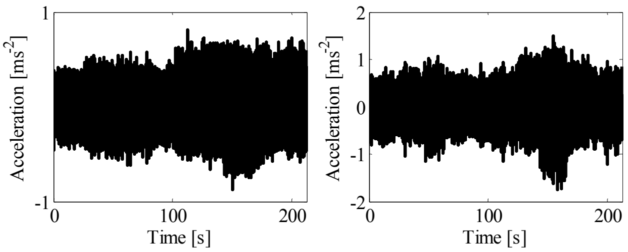

Fig. 10. Accelerations measured for time-varying engine speeds on the driver side (left) and rider side (right). The control sequence is on/off.

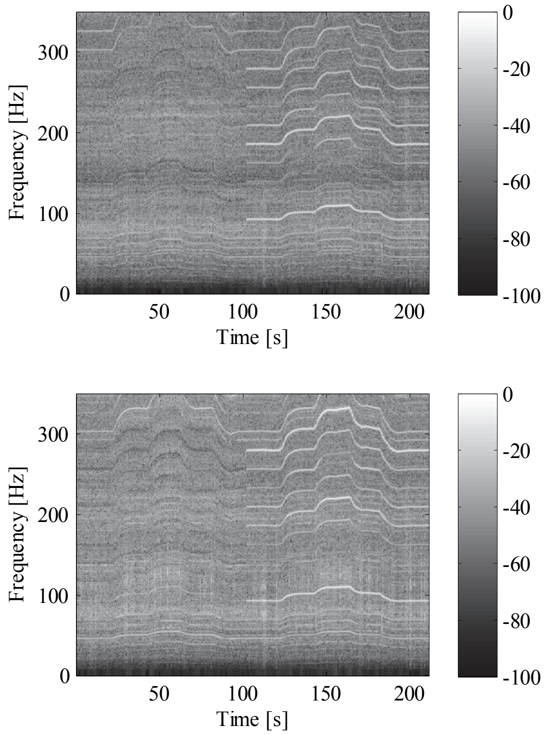

Fig. 11. Time-frequency diagram of the accelerations measured on the driver side (top) and rider side (bottom). The control sequence is on/off.

5. CONCLUSIONS

The main objective of this work was to test and develop MIMO LPV gain-scheduling controllers for the reduction of the engine-induced vibrations in a test car.

The work presented here is an extension of the previous work realized by the authors. In this paper MIMO LPV disturbance-observer gain-scheduling controllers were designed and a control switching strategy to augment the vibration reduction range is proposed. The switching strategy guarantees the stability even for fast changes of the engine speed. Triangles are used as polytopes resulting in a very simple interpolation. A simple matrix multiplication is used to calculate the LPV controller from three controller vertices.

Excellent results were achieved to increase the acoustic and vibration comfort in the vehicle even if the car did not have any acoustic or vibration problems. The reduction of the transmitted vibration when the control system was switched on was clearly noticeable in the passenger compartment.

REFERENCES

Ballesteros P. and C. Bohn. 2011a. Disturbance rejection through LPV gain-scheduling control with application to active noise cancellation. *Proceedings of the IFAC World Congress*. Milan, August 2011. 7897-902.

Ballesteros, P. and C. Bohn. 2011b. A frequency-tunable LPV controller for narrowband active noise and vibration control. *Proceedings of the American Control Conference*. San Francisco, June 2011. 1340-45.

Ballesteros, P., X. Shu, W. Heins and C. Bohn. 2013. Reduced-order two-parameter pLPV controller for the rejection of nonstationary harmonically related multisine disturbances. *Proceedings of the European Control Conference*. Zurich, July 2013. 1835-42.

Ballesteros, P., X. Shu, W. Heins, and C. Bohn. 2012. LPV gain-scheduling output feedback for active control of harmonic disturbances with time-varying frequencies. In: M. Zapateiro and F. Pozo (eds.), *Advances on Analysis and Control of Vibrations – Theory and Applications*. Rijeka, Croatia: InTech. 65-86. Available: http://dx.doi.org/10.5772/50294.

Ballesteros, P., X. Shu and C. Bohn. 2014a. Active control of engine induced vibrations in automotive vehicles through LPV gain-scheduling. *SAE 2014 World Congress*. Detroit, April 2014. Accepted for publication.

Ballesteros, P., X. Shu and C. Bohn. 2014b. A discrete-time MIMO LPV controller for the rejection of nonstationary harmonically related multisine disturbances. *Proceedings of the American Control Conference.* Portland, June 2014. Accepted for publication.

Bein, T., S. Elliot, L. Ferralli, M. Casella, J. Meschke, E. U. Saemann, F. K. Nielsen and W. Kropp. 2012. Integrated solutions for noise and vibration control in vehicles. *Procedia – Social and Behavioral Sciences* 48:919-31.

Bohn, C., A. Cortabarria, V. Härtel and K. Kowalczyk. 2003. Disturbance-observer-based active control of engine-induced vibrations in automotive vehicles. *Proceedings of the SPIE's 10th Annual International Symposium on Smart Structures and Materials*. San Diego, March 2003. 5049-68.

Bohn, C., A. Cortabarria, V. Härtel and K. Kowalczyk. 2004. Active control of engine-induced vibrations in automotive vehicles using disturbance observer gain scheduling. *Control Engineering Practice* 12:1029-39.

Darengosse, C., P. Chevrel. 2000. Linear parameter-varying controller design for active power filters. *Proceedings of the IFAC Conference on Control Systems Design*. Bratislava, June 2000. 65-70.

Du, H. and X. Shi. 2002. Gain-scheduled control for use in vibration suppression of system with harmonic excitation. *Proceedings of the American Control*

Conference. Anchorage, May 2002. 4668-69.

Du, H., L. Zhang and X. Shi. 2003. LPV technique for the rejection of sinusoidal disturbance with time-varying frequency. *IEE Proceedings on Control Theory and Applications* 150:132-38.

Duan, J., M. Li and T. C. Lim. 2013. Virtual Secondary Path Algorithm for Multichannel Active Control of Vehicle Powertrain Noise. *Journal of Vibration and Acoustics* 135: 0510141-48.

Feintuch, P. L., N. J. Bershad and A. K. Lo. 1993. A frequency-domain model for filtered LMS algorithms - Stability analysis, design, and elimination of the training mode. *IEEE Transactions on Signal Processing* 41:1518-31.

Francis, B. and W. Wonham. 1976. The internal model principle of control theory. *Automatica* 12:457-65.

Füger, T, N. Lachhab and F. Svaricek. 2012. Parameterreduktion zur Störunterdrückung mit einem diskreten LPV-Regler. *Proceedings of the Workshop of the GMA FA 1.40*. Salzburg, September 2012. (In German, Parameter reduction for disturbance rejection with a discrete-time LPV controller.)

Füger, T., N. Lachhab and F. Svaricek. 2013. Parameter reduction for disturbance attenuation with a discrete-time LPV controller. *Proceedings of the IFAC 5th Symposium on System Structure and Control (Joint Conference)*. Grenoble, France, February 2013. 791-96.

Heins, W., P. Ballesteros and C. Bohn. 2011. Gain-scheduled state-feedback control for active cancellation of multisine disturbances with time-varying frequencies. 10th MARDiH *Conference on Active Noise and Vibration Control Methods*. Wojanow, Poland, June 2011. 45-62. Available: http://www.vibrationcontrol.pl/_file/pdfs/p45.pdf.

Heins, W., P. Ballesteros and C. Bohn. 2012a. Experimental evaluation of an LPV-gain-scheduled observer for rejecting multisine disturbances with time-varying frequencies. *Proceedings of the American Control Conference*. Montreal, June 2012. 768-74.

Heins, W., P. Ballesteros, X. Shu and C. Bohn. 2012b. LPV gain-scheduled observer-based state feedback for active control of harmonic disturbances with time-varying frequencies. In: M. Zapateiro and F. Pozo (eds.), *Advances on Analysis and Control of Vibrations – Theory and Applications*. Rijeka, Croatia: InTech. 35-64. Available: http://dx.doi.org/10.5772/50293.

Inoue, T., A. Takahashi, H. Sano, M. Onishi and Y. Nakamura. 2004. NV countermeasure technology for a cylinder-on-demand engine- development of active booming noise control system applying adaptive notch filter. *Proceedings of the SAE World Congress and Exhibition*. Detroit, March 2004. SAE Technical Paper 2004-01-0411.

Kinney, C. E. and R. A. de Callafon. 2006. Scheduling control for periodic disturbance attenuation. *Proceedings of the American Control Conference*. Minneapolis, June 2006. 4788-93.

Köroğlu, H. and C. W. Scherer. 2008. LPV control for robust attenuation of non-stationary sinusoidal disturbances with measurable frequencies. *Proceedings of the 17th IFAC World Congress. Seoul*, July 2008, 4928-33.

Matsuoka, H., T. Mikasa, and H. Nemoto. 2004. NV countermeasure technology for a cylinder-on-demand engine- development of active control engine mount. *Proceedings of the SAE World Congress and Exhibition*. Detroit, March 2004. SAE Technical Paper 2004-01-0413.

Sano, H, T. Inoue, A. Takahashi, K. Terai, and Y. Nakamura. 2001. Active control system for low-frequency road noise combined with an audio system. *IEEE Transactions on Speech and Audio Processing* 9:755-63.

Sano, H., T. Yamashita and M. Nakamura. 2002. Recent application of active noise and vibration control to automobiles. *Proceedings of the ACTIVE 2002*. Southampton, July 2002. 29-42.

Shoureshi, R. and T. Knurek. 1996. Automotive applications of a hybrid active noise and vibration control. *IEEE Control Systems Magazine* 16:72–78.

Shoureshi, R. A., R. Gasser, and J. Vance. 1997. Automotive applications of a hybrid active noise and vibration control. *Proceedings of the IEEE International Symposium on Industrial Electronics*. Guimaraes, December 1997. 1071–76.

Shu, X., P. Ballesteros and C. Bohn. 2011. Active vibration control for harmonic disturbances with time-varying frequencies through LPV gain scheduling. *Proceedings of the 23rd Chinese Control and Decision Conference*. Mianyang, China, May 2011. 728-33.

Shu, X., P. Ballesteros, W. Heins and C. Bohn. 2013a. Design of structured discrete-time LPV gain-scheduling controllers through state augmentation and partial state feedback. *Proceedings of the American Control Conference*. Washington, June 2013. 6105-10.

Shu, X., W. Heins, P. Ballesteros and C. Bohn. 2013b. Two-parameter pLPV modeling of nonstationary harmonically related multisine disturbances for reduced-order gain-scheduling control. *Proceedings of the 32nd IAESTED International Conference on Modelling, Identification and Control.* Innsbruck, February 2013. 404-11.

Svaricek, F., T. Füger, H. J. Karkosch, P. Marienfeld and C. Bohn. 2010. *Automotive applications of active vibration control*. In: M. Lallart (ed.), Vibration Control. Sciyo, Croatia: InTech. 303-18. Available: http://dx.doi.org/10.5772/10149.

Witte, J., H. M. N. K. Balini and C. W. Scherer. 2010. Experimental results with stable and unstable LPV controllers for active magnetic bearing systems. *Proceedings of the IEEE International Conference on Control Applications*. Yokohama, September 2010. 950-55.